Int. J. Appl. Math. Comput. Sci., 2023, Vol. 33, No. 3, 379–394
DOI: 10.34768/amcs-2023-0027

ON THE ANALYSIS OF A MATHEMATICAL MODEL OF CAR–T CELL THERAPY FOR GLIOBLASTOMA: INSIGHTS FROM A MATHEMATICAL MODEL

MAREK BODNAR [a,*], URSZULA FORYŚ [a], MONIKA J. PIOTROWSKA [a], MARIUSZ BODZIOCH [b], JOSE A. ROMERO-ROSALES [c], JUAN BELMONTE-BEITIA [c]

[a] Institute of Applied Mathematics and Mechanics
University of Warsaw
Banacha 2, 02-097 Warsaw, Poland
e-mail: {mbodnar,urszula,monika}@mimuw.edu.pl

[b] Faculty of Mathematics and Computer Science
University of Warmia and Mazury in Olsztyn
Słoneczna 54, 10-710 Olsztyn, Poland
e-mail: mariusz.bodzioch@matman.uwm.edu.pl

[c] Mathematical Oncology Laboratory (MOLAB)
University of Castilla–La Mancha
Avda. Camilo José Cela s/n, 13071 Ciudad Real, Spain
e-mail: {joseantonio.romero,juan.belmonte}@uclm.es

Chimeric antigen receptor T (CAR-T) cell therapy has been proven to be successful against different leukaemias and lymphomas. Its success has led, in recent years, to its use being tested for different solid tumours, including glioblastoma, a type of primary brain tumour, characterised by aggressiveness and recurrence. This paper presents an analytical study of a mathematical model describing the competition of CAR-T and glioblastoma tumour cells, taking into account their immunosuppressive capacity. The model is formulated in a general way, and its basic properties are investigated. However, most of the analysis considers the model with exponential tumour growth, assuming this growth type for simplicity. The existence and stability of steady states are studied, and the subsequent focus is on two different types of treatment: constant and periodic. Finally, protocols for CAR-T cell therapy of glioblastoma are numerically derived; these are aimed at preventing the tumour from reaching a critical size and at prolonging the patients' survival time as much as possible. The analytical and numerical results provide theoretical support for the treatment of glioblastoma using CAR-T cells.

Keywords: glioblastoma, CAR-T cell therapy, mathematical modelling, periodic treatment.

1. Introduction

Cancer immunotherapy uses components of the patient's immune system to attack cancer cells selectively, and in recent years, it has come to play an important role in treating some types of cancer (D'Errico *et al.*, 2017; Koury *et al.*, 2018). One of the most promising immunotherapeutic treatments is based on the use of chimeric antigen receptor T cells, the so-called CAR-T cells. This treatment consists in extracting T cells from the patient's blood, adding an antigen receptor to them in the laboratory, subsequently re-infusing them back into the patient's body, allowing them to recognise this antigen in the tumour cells and to kill them. This type of treatment has been proven to be successful against some cancers, such as certain types of leukaemia and lymphoma (Maude *et al.*, 2018; Schuster et al., 2019).

CAR-T cells modified in the laboratory to recognise $CD19^+$ antigen have been used successfully to treat B-cell malignancies such as B leukaemia, since this antigen is expressed by B-cells and B-leukaemia cells

*Corresponding author

only. This therapy has also been reported to be successful in the treatment of acute lymphoblastic leukaemia (Feins *et al.*, 2019; Miliotou and Papadopoulou, 2018). Moreover, good results have been reported for large B-cell lymphomas (Locke *et al.*, 2019) and multiple myeloma (D'Agostino and Raje, 2020).

These successes have led to an expansion of the treatment with CAR-T cells to other types of tumours, specifically solid tumours. Thus, Brown *et al.* (2016) reported regression of glioblastoma, an aggressive primary brain tumour, under treatment with CAR-T cells. One of the differences between the way in which treatment is given in leukaemia and in glioblastoma is that in the first case, the treatment corresponds to a single initial dose, while in the second case, different cycles of doses are applied.

However, although there has been great progress in the treatment of some solid tumours with CAR-T cells, these treatments face significant challenges, as their implementation is more complicated than for non-solid tumours. For example, it is necessary to identify the corresponding tumour antigens expressed in cancerous cells but not in healthy cells (Castellarin *et al.*, 2018). The selected antigens also have to be modified to prevent the antibodies from destroying the CAR-T cells (Hege *et al.*, 2017). Finally, it should be kept in mind that the regression reported due to these treatments is often followed by relapse (Shah and Fry, 2019).

Thus, more studies are necessary in order to carry out successful CAR-T treatment in solid tumours. Here is where mathematical analysis comes into play. Mathematical models have a successful history of application in biology, medicine and oncology. In this sense, mathematical models of tumour growth provide an understanding of the tumour dynamics and its behaviour, helping in the design of optimal treatment protocols (Colli *et al.*, 2021; Garcke *et al.*, 2018; Bodnar and Piotrowska, 2016; Foryś and Marciniak-Czochra, 2003; Świerniak *et al.*, 2003; Bodzioch *et al.*, 2021; de Pillis *et al.*, 2007; Stein *et al.*, 2018; Lima *et al.*, 2022). In recent years, CAR-T cell therapies have attracted the interest of mathematicians in the study of B-cell malignancies (Mostolizadeh *et al.*, 2018) and gliomas (Sahoo *et al.*, 2020; León-Triana *et al.*, 2021). Furthermore, the use of mathematical models to understand the interaction of the immune system and tumours and to improve the prospect of immunotherapies has a long history, starting with predator-prey models which have been subsequently refined (Sancho-Araiz *et al.*, 2021).

In this paper, the reference taken is the work of León-Triana *et al.* (2021), where two mathematical models (based on differential equations) describing the treatment with CAR-T cells for glioblastoma were proposed. There a number of simulations were performed to study the interactions between tumour and CAR-T cell populations. Although the authors reported several significant results, little was said from an analytical point of view. In addition, in that work, only an initial dose of CAR-T cell treatment was considered, while this article also considers two types of treatment: constant and periodic treatment. Thus, we would like to fill the mentioned gap by making an exhaustive analytical study of the model in order to get deeper insights into the problem. Here we study the model that consists of two differential equations, while the corresponding four-dimensional differential equation model, which models dual target CAR-T cell treatment (León-Triana *et al.*, 2021), will be studied elsewhere.

The structure of the paper is as follows. Firstly, Section 2 presents the mathematical model under consideration. Next, Section 3 performs a mathematical analysis of the model including the existence, uniqueness and stability of steady states. Section 4 considers the model under an assumption of constant treatment, and Section 5 focuses on periodic treatment. Section 6 presents the parameters of the model, and Section 7 sets out a numerical study of a control problem of the model whose therapeutic goal is to maximise patient's survival time rather than to maximise the number of killed cells. Finally, Section 8 discusses the findings and summarises the conclusions.

2. Model presentation

Consider a generalised model of CAR-T cells ($\tilde{C}$) interacting with glioblastoma cells ($\tilde{T}$) that reads

$$\begin{aligned}\frac{\mathrm{d}}{\mathrm{d}s}\tilde{T} &= \left(\rho_T F(\tilde{T}) - \tilde{\alpha}_T \tilde{C}\right)\tilde{T},\\ \frac{\mathrm{d}}{\mathrm{d}s}\tilde{C} &= \tilde{\rho}_C \frac{\tilde{C}\tilde{T}}{g_T + \tilde{T}} - \tilde{\alpha}_C \frac{\tilde{C}\tilde{T}}{g_C + \tilde{C}} - \frac{1}{\tau_C}\tilde{C},\end{aligned} \tag{1}$$

where s denotes the independent (time) variable and all parameters are positive. The function F describes the tumour growth in the absence of immune response and it can have different properties. In this paper we mainly follow (León-Triana *et al.*, 2021) and assume exponential glioblastoma growth, that is $F(\tilde{T}) = \text{const}$. In general, the logistic type of the growth, with F decreasing, can also be considered for brain tumours (Pérez-García and Pérez-Romasanta, 2015; Bodnar *et al.*, 2019). Exponential growth can be valid for describing this type of tumour growth kinetics (Stensjoen *et al.*, 2015) and has the advantage of having only one adjustable parameter. More complex growth models can also describe the limited experimental data available (Stensjoen *et al.*, 2015), like Gompertzian growth which is similar to the logistic case studied here, and others have recently been proposed to be in better agreement with new metabolic and longitudinal growth data (Pérez-García

et al., 2020). However, in this article we focus on exponential and logistic growths.

Moreover, it is assumed that tumour cells are actively eliminated, with efficiency $\tilde{\alpha}_T$, by the CAR-T cells, and this interaction is modelled by the bi-linear term. In this context, ρ_T corresponds to the net growth rate (difference between proliferation and natural death rate).

On the other hand, CAR-T cell proliferation is activated as a consequence of encounters with tumour cells with a constant rate $\tilde{\rho}_C$ assuming the population half-saturation level is equal to g_T. This term is of Michaelis-Menten form, to indicate the saturated effects of the CAR-T cell response (León-Triana *et al.*, 2021; Mahlbacher *et al.*, 2019).

Inactivation of CAR-T cells is maintained by tumour cells, with a maximal inactivation rate $\tilde{\alpha}_C$ with a typical cellular half-saturation level given by g_C. There are many mechanisms leading to T-cell dysfunction in solid tumours (Anderson *et al.*, 2017). Altered signalling pathways in tumour cells help produce a suppressive tumour micro-environment enriched by inhibitory cells, which is modelled by the term $\tilde{\alpha}_C \frac{\tilde{C}\tilde{T}}{g_C+\tilde{C}}$.

The natural cell death/inactivation of activated CAR-T cells with activated CAR-T cell lifetime is also taken into account, and it is denoted by τ_C.

Finally, this model assumes that CAR-T cells would be amplified only at the tumour site, provided the tumour antigen is specific enough, and thus $\tilde{C}$ would describe the CAR-T cell population in the tumour areas.

The change of variables

$$t = s\rho_T, \quad T(t) = \frac{\tilde{T}(s)}{g_T}, \quad C(t) = \frac{\tilde{C}(s)}{g_C},$$

leads to the system

$$\begin{aligned} \dot{T} &= (f(T) - \alpha_T C)\, T, \\ \dot{C} &= \left(\frac{\rho_C T}{1+T} - \frac{\alpha_C T}{1+C} - \eta_C \right) C, \end{aligned} \tag{2}$$

where

$$\alpha_T = \frac{\tilde{\alpha}_T g_C}{\rho_T}, \quad \rho_C = \frac{\tilde{\rho}_C}{\rho_T}, \quad \alpha_C = \frac{\tilde{\alpha}_C g_T}{\rho_T g_C},$$

$$\eta_C = \frac{1}{\tau_C \rho_T}, \quad f(T) = F(\tilde{T}).$$

In general, it is assumed that f is smooth (of class $\mathbf{C}^1$), non-increasing, with $f(0) = 1$, and when considering exponential glioblastoma growth, that

Assumption A1: $f(T) \equiv 1$.

To close the system standard initial conditions are defined as

$$T(0) = T_0, \;\; C(0) = C_0, \tag{3}$$

where T_0 and C_0 are non-negative constants.

3. Model analysis

3.1. Basic properties. The local existence and uniqueness of solutions of Eqns. (2) for any initial data (3) is a consequence of the smoothness of the right-hand side of this system. Similarly, the form of this right-hand side ensures global existence and non-negativity of solutions.

3.2. Existence of steady states. To designate the steady states of Eqns. (2), possible intersections of T-null-cline, given by $T = 0$ or $C = f(T)/\alpha_T$, with C-null-cline given by $C = 0$ or

$$\frac{\rho_C T}{1+T} - \frac{\alpha_C T}{1+C} - \eta_C = 0$$

were studied.

It is easy to see that Eqns. (2) always have one steady state $(0,0)$, which is a saddle (with the T-axis being an unstable manifold and the C-axis being a stable one). Clearly, the number of non-negative steady states strongly depends on the form of the function f and thus it is hard to formulate conditions guaranteeing the existence of a given number of them. Nevertheless, particular results can be provided under Assumption A1.

We now focus on the non-trivial part of the C-null-cline and treat it as a function of T, that is,

$$C = g(T) = \frac{\alpha_C T(1+T)}{(\rho_C - \eta_C)T - \eta_C} - 1,$$

and consider two mutually exclusive cases: $\rho_C \le \eta_C$ and $\rho_C > \eta_C$.

Lemma 1. *Let Assumption A1 be satisfied. For $\rho_C \le \eta_C$, Eqns.* (2) *have exactly one non-negative steady state (0,0), while for $\rho_C > \eta_C$, Eqns.* (2) *have additionally*

- *two positive steady states for*

$$\alpha_C < \alpha_C^{\mathrm{crit}} := \left(\frac{1}{\alpha_T} + 1 \right) \left(\sqrt{\rho_C} - \sqrt{\eta_C} \right)^2; \tag{4}$$

- *one positive steady state for $\alpha_C = \alpha_C^{\mathrm{crit}}$;*
- *no positive steady state for $\alpha_C > \alpha_C^{\mathrm{crit}}$.*

Proof. Assumption A1 indicates that the non-trivial part of T-null-cline is given by $\alpha_T C = 1$. For $\rho_C \le \eta_C$ we have $g(T) < 0$ for any $T \ge 0$. Hence, there is no positive steady state of Eqns. (2) and the system has only one steady state $(0,0)$.

On the other hand, for $\rho_C > \eta_C$ we have $g(T) < 0$ for $T < \frac{\eta_C}{\rho_C - \eta_C} := T_{\mathrm{as}}$. Calculating the derivative of g gives

$$g'(T) = \alpha_C \frac{(\rho_C - \eta_C)T^2 - 2\eta_C T - \eta_C}{\left((\rho_C - \eta_C)T - \eta_C\right)^2}.$$

Note that g' has one positive zero as the free term in the numerator is negative. The discriminant of the numerator is equal to $4\eta_C^2 + 4\eta_C(\rho_C - \eta_C) = 4\eta_C\rho_C$ and thus the positive root of g' is equal to

$$\frac{2\eta_C + \sqrt{4\eta_C\rho_C}}{2(\rho_C - \eta_C)} = \frac{\sqrt{\eta_C}}{\sqrt{\rho_C} - \sqrt{\eta_C}} := T_{\min}.$$

It is easy to see that $T_{\min} > T_{\text{as}}$ and the function g has a minimum at $T_{\min}$. Clearly, the limit of g as $T \to T_{\text{as}}^+$ is equal to $+\infty$, g decreases on the interval $(T_{\text{as}}, T_{\min})$ and increases to $+\infty$ for $T > T_{\min}$. Moreover, we have

$$g_{\min} := g(T_{\min}) = \frac{\alpha_C}{\left(\sqrt{\rho_C} - \sqrt{\eta_C}\right)^2} - 1.$$

Thus, two positive steady states exist if and only if $g_{\min} < 1/\alpha_T$, which concludes the proof after some algebraic manipulations. ■

Note that for $g_{\min} \leq 0$, Eqns. (2) have two positive steady states, while for $g_{\min} > 0$, i.e., $\alpha_C > \left(\sqrt{\rho_C} - \sqrt{\eta_C}\right)^2$, the existence of positive steady states depends on the magnitude of α_T.

3.3. Stability of the steady states. To study the local the stability of the steady states, we calculate the Jacobian matrix of Eqns. (2):

$$J(T, C) = \begin{pmatrix} f(T) - \alpha_T C + T f'(T) & -\alpha_T T \\ \left(\frac{\rho_C}{(1+T)^2} - \frac{\alpha_C}{1+C}\right) C & \frac{\rho_C T}{1+T} - \frac{\alpha_C T}{1+C} - \eta_C + \frac{\alpha_C TC}{(1+C)^2} \end{pmatrix}.$$

Clearly, the trivial steady state is a saddle with the characteristic values $\lambda_1 = f(0) = 1$, $\lambda_2 = -\eta_C$.

On the other hand, for any positive steady state $(\bar{T}, \bar{C})$ we have

$$f(\bar{T}) - \alpha_T \bar{C} = 0, \quad \frac{\rho_C \bar{T}}{1+\bar{T}} - \frac{\alpha_C \bar{T}}{1+\bar{C}} - \eta_C = 0.$$

Hence

$$J(\bar{T}, \bar{C}) = \begin{pmatrix} \bar{T} f'(\bar{T}) & -\alpha_T \bar{T} \\ \left(\frac{\rho_C}{(1+\bar{T})^2} - \frac{\alpha_C}{1+\bar{C}}\right) \bar{C} & \frac{\alpha_C \bar{T}\bar{C}}{(1+\bar{C})^2} \end{pmatrix},$$

with

$$\operatorname{tr} J(\bar{T}, \bar{C}) = \frac{\alpha_C \bar{T}\bar{C}}{(1+\bar{C})^2} + \bar{T} f'(\bar{T}).$$

Clearly, if Assumption A1 is met, then $f'(T) \equiv 0$; thus $\operatorname{tr} J(\bar{T}, \bar{C}) > 0$, and therefore all the existing positive steady state(s) must be unstable.

Assume now that, under Assumption A1, Eqns. (2) have two positive steady states, $(\bar{T}_1, \bar{C})$, $(\bar{T}_2, \bar{C})$, with $T_1 < T_2$, i.e., (4) holds. Then $T_1 < T_{\min} < T_2$, and thus

$$\begin{aligned} \det J(\bar{T}_1, \bar{C}) &> \alpha_T \bar{T}_1 \bar{C} \left(\frac{\rho_C}{(1+\bar{T}_{\min})^2} - \frac{\alpha_C}{1+\bar{C}} \right) \\ &= \alpha_T \bar{T}_1 \bar{C} \left((\sqrt{\rho_C} - \sqrt{\eta_C})^2 - \frac{\alpha_C}{1+\bar{C}} \right) \\ &> 0, \end{aligned}$$

due to (4) bearing in mind that $\alpha_T \bar{C} = 1$.

Now, it will be proven that the steady state $(\bar{T}_2, \bar{C})$ is a saddle point if it exists. It is shown that $\det J(\bar{T}_2, \bar{C}) < 0$. To this end, it is necessary to calculate $\bar{T}_2$. Rearranging $g(\bar{T}_2) = 1/\alpha_T$ gives

$$\alpha_C \bar{T}^2 + \left(\alpha_C - (1+\bar{C})(\rho_C - \eta_C)\right) \bar{T} + \eta_C(1+\bar{C}) = 0,$$

for which the discriminant is

$$\begin{aligned} \Delta &= \left(\alpha_C - (1+\bar{C})(\rho_C - \eta_C)\right)^2 - 4\alpha_C \eta_C (1+\bar{C}) \\ &= \alpha_C^2 - 2\alpha_C(1+\bar{C})(\rho_C + \eta_C) \\ &\quad + (1+\bar{C})^2(\rho_C - \eta_C)^2, \end{aligned}$$

and the greater root has the following form:

$$\bar{T}_2 = \frac{-\alpha_C + (1+\bar{C})(\rho_C - \eta_C) + \sqrt{\Delta}}{2\alpha_C}.$$

Clearly, $\det J(\bar{T}_2, \bar{C}) < 0$ iff

$$\frac{\rho_C}{(1+\bar{T}_2)^2} < \frac{\alpha_C}{1+\bar{C}} \;\Leftrightarrow\; (1+\bar{T}_2)^2 > \frac{\rho_C(1+\bar{C})}{\alpha_C},$$

which is equivalent to

$$\left(\alpha_C + (1+\bar{C})(\rho_C - \eta_C) + \sqrt{\Delta}\right)^2 > 4\alpha_C \rho_C (1+\bar{C}).$$

Expanding the first bracket, using the definition of Δ and doing some algebraic manipulation, gives

$$\Delta > -\left(\alpha_C + (1+\bar{C})(\rho_C - \eta_C)\right)\sqrt{\Delta},$$

which holds whenever $\rho_C - \eta_C > 0$, and there are two positive steady states, as then $\Delta > 0$.

Corollary 1. *On Assumption A1, if $\rho_C > \eta_C$ and Eqn.* (4) *is satisfied, then the trivial steady state of Eqns.* (2) *is a saddle. Moreover, Eqns.* (2) *have two positive steady states $S_1 = (\bar{T}_1, \bar{C})$, $S_2 = (\bar{T}_2, \bar{C})$, with $\bar{T}_1 < \bar{T}_2$, S_2 being a saddle point, while S_1 is an unstable node or focus.*

Remark 1. If Assumption A1 is met, then Eqns. (2) have no periodic orbit in the phase space $\mathbb{R}^2_+$.

Proof. Using the Dulac–Bendixson criterion

$$\frac{\partial}{\partial T}\left(\frac{1}{TC}(1-\alpha_T C)T\right) + \frac{\partial}{\partial C}\left(\frac{1}{TC}\left(\frac{\rho_C T}{1+T}-\frac{\alpha_C T}{1+C}-\eta_C\right)C\right) = \frac{\alpha_C}{(1+C)^2} > 0.$$

Hence, there is no periodic orbit for T, $C > 0$. As a consequence, the Dulac–Bendixson criterion guarantees the absence of closed invariant orbits. ■

The instability of all steady states, together with the lack of periodic solutions, implies that the solutions, to Eqn. (2) are unbounded. Phase portrait analysis indicates that, with increasing time, T tends to infinity while C goes to 0. This means that in the case of a single dose administration the tumour eventually will regrow and later on increase in size exponentially, while CAR-T cells will be eliminated. Although it happens independently of the parameters, depending on the value of α_C, the inactivation parameter of CAR-T cells by tumour cells, such regrowth could be faster or slower, as long as it is not zero. This term prevents the system from ever reaching a periodic solution, which could be expected in a more standard predator-prey model. Furthermore, this parameter indicates whether, for a given number of T cells, they will tend to zero independently of the tumour size.

For the generalised logistic tumour growth the situation is more complex. Equations (2) may have up to four non-negative steady states: $(0,0)$, $(K,0)$ (where K is a carrying capacity for tumour), and up to two positive steady states (the null-cline of C is a convex function of T, while the null-cline for T is a line so they have at most two intersections). Among them, $(0,0)$ is a saddle point while stability conditions of the other steady states are complex.

4. Model with constant treatment

The analysis presented in Section 3 indicates that there is no possibility of curing a patient using a single boost of CAR-T cells. Thus, consider the model with a constant influx $A > 0$ of these cells, namely

$$\begin{aligned}\dot{T} &= (f(T)-\alpha_T C)\,T,\\ \dot{C} &= \left(\frac{\rho_C T}{1+T}-\frac{\alpha_C T}{1+C}-\eta_C\right)C + A.\end{aligned} \tag{5}$$

The null-cline for T does not change compared with the case $A = 0$, while calculating the C-null-cline gives

$$\left(\frac{\rho_C T}{1+T}-\frac{\alpha_C T}{1+C}-\eta_C\right)C = -A \tag{6}$$

which in $\mathbb{R}^2_+$ is equivalent to the quadratic equation

$$h(T)C^2 - b(T)C + A = 0, \tag{7}$$

where

$$b(T) = \alpha_C T - A - h(T), \quad h(T) = \frac{\rho_C T}{1+T} - \eta_C,$$

h is continuous and increasing from $-\eta_C$ for $T = 0$ to $\rho_C - \eta_C$ for $T \to +\infty$. Because Eqn. (7) is quadratic in C, for each $T \geq 0$, there exist at most two solutions $C(T)$. The shape of the C-null-cline strongly depends on the model parameters, as discussed below.

Proposition 1. *If Assumption A1 is met and $\rho_C \leq \eta_C$, then for every $T \geq 0$, Eqn. (7) defines a unique curve $\hat{C}(T)$ in $\mathbb{R}^2_+$ and $\hat{C} \to 0$ as $T \to \infty$. Moreover, if $A \leq A_{\rm th} := \eta_C\left(\frac{\alpha_C}{\rho_C}-1\right)$, then the function $\hat{C}$ is decreasing for all $T > 0$, while for $A > A_{\rm th}$ there exists $\hat{T}_1 > 0$ such that the function $\hat{C}$ increases for $T \in [0, \hat{T}_1)$ and decreases for $T > \hat{T}_1$.*

Proof. Note that, if $\rho_C \leq \eta_C$, then $h(T) < 0$ for all $T \geq 0$. As the free term of Eqn. (7) is positive, there exists a unique positive solution $\hat{C}(T)$ defined for all $T \geq 0$, namely

$$\hat{C}(T) = \frac{b(T) - \sqrt{b^2(T) - 4Ah(T)}}{2h(T)} \quad \text{for} \quad T > 0. \tag{8}$$

For $T = 0$ Eqn. (6), as well as Eqn. (7), is equivalent to $\eta_C C = A$, that is $\hat{C}(0) = A/\eta_C$. Using the Implicit Function Theorem and calculating the derivative $\hat{C}'(T) = \mathrm{d}\hat{C}/\mathrm{d}T$ gives

$$\hat{C}'(T) = \frac{\hat{C}(T)\Big(\alpha_C - h'(T)\big(1+\hat{C}(T)\big)\Big)}{\big(2\hat{C}(T)+1\big)h(T) - \alpha_C T + A},$$
$$h'(T) = \frac{\rho_C}{(1+T)^2}.$$

Using the identity $\hat{C}(0) = A/\eta_C$ gives

$$\hat{C}'(0) = \frac{A}{\eta_C}\frac{\rho_C\left(1+\frac{A}{\eta_C}\right)-\alpha_C}{\eta_C + A}.$$

Thus, $\hat{C}'(0) < 0$ for $A < A_{\rm th}$ and $\hat{C}'(0) > 0$ for $A > A_{\rm th}$.

Note that Eqn. (6) can be alternatively expressed as a quadratic equation in T, that is,

$$\frac{\alpha_C C}{1+C}T^2 + \left(\frac{\alpha_C C}{1+C} - \rho_C C + \eta_C C - A\right)T + \eta_C C - A = 0, \tag{9}$$

meaning that for each $\bar{C} > 0$ there exist at most two positive solutions (T_1 and T_2) of Eqn. (9), such that $\bar{C} = \hat{C}(T_1) = \hat{C}(T_2)$. Moreover,

$$\lim_{T\to+\infty} \hat{C}(T) = \lim_{T\to+\infty} \frac{2A}{b(T) + \sqrt{b^2(T) - 4Ah(T)}} = 0.$$

Assume $A < A_{\rm th}$. Then $\hat{C}'(0) < 0$. If $\hat{C}$ is non-decreasing, it must have at least one minimum and one maximum, as it goes to 0 at $T \to \infty$. However, in this case, for each $\bar{C} \in (C_{\min}, C_{\max})$, where $C_{\min}$ is a first local minimum and $C_{\max}$ is another local maximum, there exist three points T_i, $i = 1, 2, 3$, such that $\bar{C} = \hat{C}(T_i)$ which contradicts the fact that there could be only two such points. If $A = A_{\rm th}$ then $\hat{C}'(0) = 0$, $\hat{C}'(T) < 0$ for T close to 0 and the above arguments hold.

An analogous argument proves that, if $A > A_{\rm th}$, then there exist $\hat{T}_1 > 0$ such that the function $\hat{C}$ increases for $T \in [0, \hat{T}_1)$ and decreases for $T > \hat{T}_1$. ■

Proposition 2. *If Assumption A1 is met and $\rho_C > \eta_C$, then there is a threshold value*

$$T_{\rm as} = \frac{\eta_C}{\rho_C - \eta_C}$$

such that for $T < T_{\rm as}$ Eqn. (7) *defines a unique curve $\hat{C}(T)$, while for $T > T_{\rm as}$, if the C-null-cline is defined, then there are two solutions, $\hat{C}(T)$ (defined by* (8)*) and*

$$\tilde{C}(T) = \frac{b(T) + \sqrt{b^2(T) - 4Ah(T)}}{2h(T)}, \qquad (10)$$

which form two branches of this null-cline located in $\mathbb{R}^2_+$ as shown in Fig. 1. The monotonicity of each branch can change at most once. Moreover, $\hat{C} \to 0$, while $\tilde{C} \to \infty$ linearly with T, as $T \to \infty$.

Proof. First note that for $T < T_{\rm as}$, $h(T) < 0$ and the free term of Eqn. (7) is positive meaning that there is a unique positive solution defined by (8). Moreover,

1. Case 1: if $A \geq \alpha_C T_{\rm as}$, then $\lim\limits_{T\to T_{\rm as}^-} \hat{C}(T) = \infty$;
2. Case 2: if $A < \alpha_C T_{\rm as}$, then $\lim\limits_{T\to T_{\rm as}^-} \hat{C}(T) = \frac{A}{\alpha_C T_{\rm as} - A}$.

Two positive solutions of Eqn. (7) (given by (8) and (10)) exist for $T > T_{\rm as}$ iff $b(T) > 0$ and $4Ah(T) < b^2(T)$.

In Case 1 there is no solution of Eqn. (7) for $T > T_{\rm as}$ near T_{as}; cf. Fig. 1(a). In Case 2 we have $b(T_{\rm as}) > 0$ and $\lim_{T\to T_{\rm as}^+} \tilde{C}(T) = \infty$. Because b and h are continuous, there are two solutions of Eqn. (7) for $T > T_{\rm as}$ near $T_{\rm as}$; cf. Fig. 1(b) and (c). In both cases for sufficiently large T we have $b(T) > 0$ and $b^2(T) > 4Ah(T)$. Hence, there are two solutions, $\hat{C}$ and $\tilde{C}$, and $\hat{C}$ tends to 0, while

$$\lim_{T\to\infty} \frac{\tilde{C}}{T} = \frac{\alpha_C}{\rho_C - \eta_C},$$

that is, $\tilde{C}$ tends to $+\infty$ linearly. Figure 1 shows three possible graphs of both branches of the C-null-cline.

Due to Eqn. (9), the same argument as in the proof of Proposition 1 shows that the situation with two positive solutions of Eqn. (7) existing for some interval (T_1, T_2) and disappearing at T_1 and T_2 is not possible. Moreover, the part of the C-null-cline that satisfies $C < A/\eta_C$ is decreasing, and each branch of the C-null-cline can change its monotonicity at most once. ■

4.1. Steady states for $A > 0$. In the case of constant treatment there is always a semi-trivial steady state $(0, \check{C})$ with $\check{C} = A/\eta_C$. Moreover, if Assumption A1 is met, then any positive steady state $(\bar{T}, 1/\alpha_T)$ satisfies

$$\gamma T^2 + \Big(\gamma - \rho_C + \eta_C - \alpha_T A\Big)T + \eta_C - A\alpha_T = 0, \quad (11)$$

with

$$\gamma = \frac{\alpha_C \alpha_T}{1 + \alpha_T}$$

and thus there are at most two positive steady states.

Theorem 1. *If Assumption A1 is met and $A > A_{\rm crit} = \eta_C/\alpha_T$, then there is exactly one positive steady state of Eqns.* (5) *which is a saddle, while the semi-trivial steady state is a stable node.*

Proof. Under the assumptions of this theorem the free term in (11) is negative. Hence (11) has only one positive solution.

The Jacobian matrix of Eqns. (5) is the same as for $A = 0$:

$$J(0, \check{C}) = \begin{pmatrix} 1 - \frac{\alpha_T A}{\eta_C} & 0 \\ \left(\rho_C - \frac{\alpha_C}{1 + \frac{A}{\eta_C}}\right)\frac{A}{\eta_C} & -\eta_C \end{pmatrix},$$

implying that for $A > A_{\rm crit}$ the semi-trivial steady state is a stable node.

For the positive steady state $(\bar{T}, \bar{C})$, where $\bar{C} = 1/\alpha_T$, we have

$$\frac{\rho_C \bar{T}}{1 + \bar{T}} - \frac{\alpha_C \bar{T}}{1 + \bar{C}} - \eta_C = -A\alpha_T.$$

Hence

$$J(\bar{T}, \bar{C}) = \begin{pmatrix} 0 & -\alpha_T \bar{T} \\ \left(\frac{\rho_C}{(1+\bar{T})^2} - \frac{\alpha_C}{1+\bar{C}}\right)\bar{C} & \frac{\alpha_C \bar{T}\bar{C}}{(1+\bar{C})^2} - A\alpha_T \end{pmatrix}.$$

Using identity $\alpha_T \bar{C} = 1$ and the definition of γ gives

$$\det J(\bar{T}, \bar{C}) = \bar{T}\left(\frac{\rho_C}{(1+\bar{T})^2} - \gamma\right) < 0$$

whenever

$$\rho_C < \gamma(1 + \bar{T})^2. \qquad (12)$$

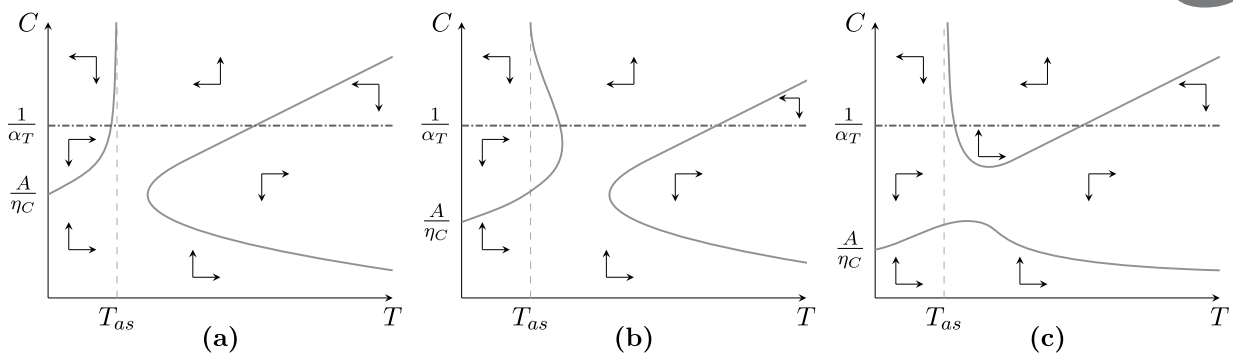

Fig. 1. Phase portrait sketches with all possible graphs of the C-null-cline (solid line) and the T-null-cline for an arbitrarily chosen α_T (dash-dotted line) of Eqns. (5) for $\eta_C < \rho_C$. The T-null-cline will move up and down with a decrease and increase in α_T, respectively. Panel (a) illustrates Case 1 from the proof of Proposition 2 ($A \geq \alpha_C T_{\text{as}}$). Panels (b) and (c) reflect the possible situations for Case 2 from the proof of Proposition 2 ($A < \alpha_C T_{\text{as}}$). The C-null-cline looks as in the panel (b) if $4Ah(T) > b^2(T)$ for some $T > T_{\text{as}}$, while if $4Ah(T) < b^2(T)$ for all $T > T_{\text{as}}$, the C-null-cline looks as on the panel (c).

From (11), under the assumptions of this theorem,

$$1 + \bar{T} = \frac{\gamma + \rho_C - \eta_C + \alpha_T A + \sqrt{\Delta}}{2\gamma},$$

where

$$\Delta = \left(\gamma - \rho_C + \eta_C - \alpha_T A\right)^2 + 4\gamma\left(A\alpha_T - \eta_C\right) > 0.$$

Rewriting (12) as

$$4\gamma\rho_C < \left(\gamma + \rho_C - \eta_C + \alpha_T A + \sqrt{\Delta}\right)^2,$$

we obtain

$$\begin{aligned} 0 < &(\gamma - \rho_C)^2 + \left(\alpha_T A - \eta_C + \sqrt{\Delta}\right)^2 \\ &+ 2\left(\gamma + \rho_C\right)\left(\alpha_T A - \eta_C + \sqrt{\Delta}\right), \end{aligned}$$

which always holds under the assumptions of this theorem. ■

Theorem 2. *If Assumption A1 is met and $A < A_{\text{crit}}$, then for*

$$\begin{aligned} A > \bar{A} &= A_{\text{crit}} - \frac{\rho_C - \gamma\left(1 + 2\max\left\{0, \sqrt{\frac{\rho_C}{\gamma}} - 1\right\}\right)}{\alpha_T} \end{aligned}$$

there are two positive steady states of Eqns. (5)*, while for $A < \bar{A}$ there is no positive steady state.*

Proof. If $A < A_{\text{crit}}$, then the free term of Eqn. (11) is positive. Thus, to have two positive steady states, it is necessary that the coefficient of the linear term is negative, that is,

$$x := \eta_C - \alpha_T A < \rho_C - \gamma. \tag{13}$$

The discriminant of Eqn. (11) is positive if

$$P(x) := (\gamma - \rho_C + x)^2 - 4\gamma x > 0,$$

while the discriminant of the polynomial P is

$$\Delta_P = 4(\gamma + \rho_C)^2 - 4(\gamma - \rho_C)^2 = 16\rho_C\gamma > 0,$$

implying that there are two positive zeros of P, namely

$$x_{1,2} = \gamma + \rho_C \mp 2\sqrt{\gamma\rho_C} = \left(\sqrt{\gamma} \mp \sqrt{\rho_C}\right)^2.$$

Thus, the condition guaranteeing the existence of two positive steady states of Eqns. (5) becomes $\eta_C - A\alpha_T < x_1$ or $\eta_C - A\alpha_T > x_2$. Combining this with (13), we get

$$\eta_C - A\alpha_T < \rho_C + \min\left\{-\gamma, \gamma - 2\sqrt{\gamma\rho_C}\right\}$$

or

$$\gamma + \rho_C + 2\sqrt{\gamma\rho_C} < \eta_C - A\alpha_T < \rho_C - \gamma.$$

Note that the second condition is contradictory, while the first is equivalent to

$$A\alpha_T > \eta_C - \rho_C + \gamma + 2\gamma\max\left\{0, -1 + \sqrt{\frac{\rho_C}{\gamma}}\right\},$$

which completes the proof. ■

Theorem 3. *Let Assumption A1 be met. If $\eta_C \leq \rho_C - \sqrt{\gamma\rho_C}$ and $A < A_{\text{crit}}$, then the positive steady state $(\bar{T}, \bar{C})$ of Eqns.* (5) *with $\bar{T} < T_{\text{as}}$ is locally asymptotically stable.*

Proof. To prove the theorem means to prove that $\operatorname{tr} J(\bar{T}, \bar{C}) < 0$ and $\det J(\bar{T}, \bar{C}) > 0$. But

$$\bar{T} < \frac{\eta_C}{\rho_C - \eta_C} = T_{\text{as}} < \frac{A}{\alpha_C}$$

gives

$$\begin{aligned}\operatorname{tr} J(\bar{T},\bar{C}) &= \frac{\alpha_T}{(1+\alpha_T)^2}\Big(\alpha_C\bar{T} - A(1+\alpha_T)^2\Big)\\ &< \frac{\alpha_T}{(1+\alpha_T)^2}\Big(\alpha_C T_{\rm as} - A(1+\alpha_T)^2\Big)\\ &< \frac{\alpha_T}{(1+\alpha_T)^2}\Big(A - A(1+\alpha_T)^2\Big) < 0,\\ \det J(\bar{T},\bar{C}) &= \alpha_T\bar{T}\bar{C}\left(\frac{\rho_C}{(1+\bar{T})^2} - \gamma\right)\\ &> \alpha_T\bar{T}\bar{C}\left(\frac{(\rho_C-\eta_C)^2}{\rho_C} - \gamma\right)\\ &= \alpha_T\bar{T}\bar{C}\left(\frac{(\rho_C-\eta_C)^2 - \gamma\rho_C}{\rho_C}\right) \ge 0\end{aligned}$$

as, due to the assumption, $\rho_C - \eta_C - \sqrt{\gamma\rho_C} \ge 0$. ■

Proposition 3. *Let Assumption A1 be met and* $(\bar{T},\bar{C})$ *be a positive steady state of Eqns.* (5)*. Set*

$$T_{\rm crit} = \min\left\{\frac{A(1+\alpha_T)^2}{\alpha_C}, \sqrt{\frac{\rho_C}{\gamma}} - 1\right\}.$$

Then

1. *for* $\bar{T} < T_{\rm crit}$ *the steady state* $(\bar{T},\bar{C})$ *is locally asymptotically stable;*
2. *for* $\bar{T} > T_{\rm crit}$ *the steady state* $(\bar{T},\bar{C})$ *is unstable.*

Proof. Inequality $\operatorname{tr} J(\bar{T},\bar{C}) < 0$ is equivalent to $\alpha_C\bar{T} < A(1+\alpha_T)^2$. Similarly, inequality $\det J(\bar{T},\bar{C}) > 0$ is equivalent to $\rho_C > \gamma(1+\bar{T})^2$, and thus, the assertion of the theorem follows. ■

The value of $T_{\rm crit}$ gives a condition to keep the tumour under control. It also provides a threshold for which the tumour will be controlled, since for a sufficiently large A the value of the tumour steady state will be low and $T_{\rm crit}$ will become independent of A. Figure 2 shows the tumour size T at a steady state and summarises the analytical results obtained in Theorems 1–3 and Proposition 3. For small values of A, both the steady states are unstable or do not exist.

Finally, we would like to emphasize that constant treatment is a first approximation to a more realistic periodic treatment, which will be studied in the following section.

5. Periodic treatment

This section considers Eqns. (2) with a general tumour growth, assuming that a portion m of CAR-T cells is injected each time $t_n = nP$, where P is a given positive constant. Specifically, T and C satisfy Eqns. (2) for $t \in [t_n, t_{n+1})$ and

$$T(t_n) = \lim_{t\to t_n^-} T(t), \quad C(t_n) = \lim_{t\to t_n^-} C(t) + m. \quad (14)$$

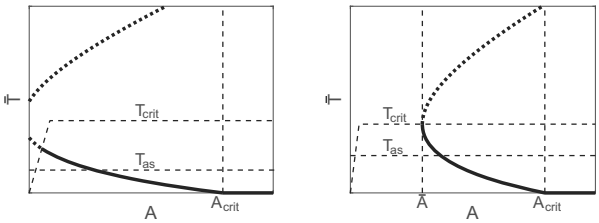

(a) (b)

Fig. 2. Tumour size at a steady state. The solid lines depict stable steady states, while the dotted lines indicate unstable steady states. Panel (a) illustrates the situation when $\bar{A} < 0$, while (b) reflects $\bar{A} > 0$.

In this case, Eqns. (2) together with (14) will be referred to as impulsive Eqns. (2).

From a medical point of view, it is interesting to note that Brown *et al.* (2016) reported glioblastoma regression using CAR-T cells with (almost) periodic treatment, meaning the following: CAR-T cells were delivered every 7 days, with 1 week of rest after cycles 3 and 6 for evaluation of safety and disease. Thus, this treatment will be modelled in what follows (without taking of the account rest).

Theorem 4. *There exists a periodic solution of impulsive Eqns.* (2) *that has the form*

$$\big(0, C^*(t)\big), \quad C^*(t) = \frac{m}{1-\mathrm{e}^{-\eta_C P}}\,\mathrm{e}^{-\eta_C(t-nP)}, \ \ n\in\mathbb{N},$$

which is locally stable for

$$A_{\rm crit} < \frac{m}{P}. \quad (15)$$

Proof. If $T_0 = 0$, then $T(t) \equiv 0$ and for C we have an impulsive equation of the following form:

$$\begin{aligned}\dot{C} &= -\eta_C C \quad \text{for } nP \le t < (n+1)P,\\ C(nP) &= \lim_{t\to nP^-} C(t) + m, \quad n\in\mathbb{N}.\end{aligned} \quad (16)$$

Clearly, $C^*(t)$ satisfies $\dot{C}^*(t) = -\eta_C C^*(t)$. Moreover

$$\begin{aligned}\lim_{t\to nP^-} C^*(t) + m &= \frac{m\,\mathrm{e}^{-\eta_C P}}{1-\mathrm{e}^{-\eta_C P}} + m\\ &= \frac{m}{1-\mathrm{e}^{-\eta_C P}} = C^*(nP).\end{aligned}$$

Thus, $\big(0, C^*(t)\big)$ fulfils (16).

To find conditions for the local stability of this periodic solution, we expand the coordinates of the solution around the periodic solution; that is, rewrite these coordinates as

$$T = \varepsilon T_1 + O(\varepsilon^2), \quad C = C^* + \varepsilon C_1 + O(\varepsilon^2), \ \ \varepsilon \ll 1,$$

Table 1. Parameters for the model described by Eqns. (1). For detailed description and estimation, see the work of León-Triana *et al.* (2021). In the fifth column the values of parameters used in the simulations are given. The last three columns show the values of Pearson's correlation coefficients, which describe the dependence of the changes in a given parameter on the time in which the tumour reaches a critical size, when all other parameters are on the left, middle and right ends of the ranges. The symbol '*' indicates the correlation coefficient for which the corresponding p-value is less than 0.05.

Param.	Ranges	Units	Refs.	Value	min	mid	max
$\tilde{\rho}_C$	$0.2-0.9$	day^{-1}	Stein *et al.*, 2019	0.9	0.71^*	1.00^*	1.00^*
g_T	10^7-10^{10}	cell	Stein *et al.*, 2019	10^{10}	-1.00^*	-1.00^*	-1.00^*
$\tilde{\alpha}_C$	$0.01-0.99$	day^{-1}	Radunskaya *et al.*, 2018	0.035	-0.59	-0.99^*	-1.00^*
g_C	$5\times10^8-5\times10^9$	cell	Radunskaya *et al.*, 2018	2×10^9	0.99^*	0.94^*	0.94^*
τ_C	$7-30$	day	Ghorashian *et al.*, 2019	7	0.94^*	0.92^*	0.92^*
ρ_T	$0.001-0.2$	day^{-1}	Stein *et al.*, 2019	0.01	-0.57	-0.57	-0.57
$\tilde{\alpha}_T$	$10^{-12}-5\times10^{-10}$	$\text{day}^{-1}\text{cell}^{-1}$	León-Triana *et al.*, 2021	5×10^{-10}	1.00^*	1.00^*	1.00^*

and consider the (T_1, C_1)-system of the first-order approximation

$$\begin{aligned}\dot{T}_1 &= (1-\alpha_T C^*)\,T_1,\\ \dot{C}_1 &= -\eta_C C_1 + \rho_C C^* T_1 - \frac{\alpha_C C^*}{1+C^*}T_1.\end{aligned} \tag{17}$$

Let $\Phi(t)$ denote the fundamental matrix of Eqns. (17). To find this matrix, it is necessary to calculate the solutions of Eqns. (17) for initial datum $(1,0)$ and $(0,1)$. It is easy to see that for the second initial data $(0,1)$

$$T_1 \equiv 0 \quad\Longrightarrow\quad \dot{C}_1 = -\eta_C C_1 \quad\Longrightarrow\quad C_1(t) = \mathrm{e}^{-\eta_C t}.$$

This means that the fundamental matrix is upper triangular and therefore, to find Floquet multipliers it is enough to find T_1 for the first initial datum $(1,0)$.

Let $t \in [nP, (n+1)P)$. Calculate

$$\int\limits_{T_1(nP)}^{T_1(t)} \frac{\mathrm{d}T_1}{T_1} = \int\limits_{nP}^{t} (1-\alpha_T C^*(s))\,\mathrm{d}s.$$

Thus,

$$\ln\frac{T_1(t)}{T_1(nP)} = t - nP - \frac{m}{A_{\text{crit}}}\cdot\frac{1-\mathrm{e}^{-\eta_C(t-nP)}}{1-\mathrm{e}^{-\eta_C P}},$$

and eventually

$$\begin{aligned}T_1(t) = T_1(nP)\cdot\exp\Bigg(t - nP - \frac{m}{A_{\text{crit}}}\\ \cdot\frac{1-\mathrm{e}^{-\eta_C(t-nP)}}{1-\mathrm{e}^{-\eta_C P}}\Bigg),\end{aligned} \tag{18}$$

for $t \in [nP, (n+1)P)$. Hence,

$$\Phi(t) = \begin{pmatrix} T_1(nP)\cdot\exp\left(t-nP-\frac{m}{A_{\text{crit}}}\cdot\frac{1-\mathrm{e}^{-\eta_C(t-nP)}}{1-\mathrm{e}^{-\eta_C P}}\right) & \star \\ 0 & \mathrm{e}^{-\eta_C t}\end{pmatrix},$$

where $\star$ means a term that is not relevant and thus the monodromy matrix is

$$\Phi(P) = \begin{pmatrix} \mathrm{e}^{P-\frac{m}{A_{\text{crit}}}} & \star \\ 0 & \mathrm{e}^{-\eta_C P}\end{pmatrix}$$

and the Floquet multipliers are given by

$$\lambda_1 = \mathrm{e}^{P-\frac{m}{A_{\text{crit}}}}, \quad \lambda_2 = \mathrm{e}^{-\eta_C P},$$

For both of these to be less than 1, it is necessary to assume $P < m/A_{\text{crit}}$. ■

Note that when considering exponential tumour growth the condition for the stability of the periodic orbit for the impulsive system is the same as the condition of stability of the semi-trivial steady state for the system with constant treatment under the assumption

$$A = \frac{m}{P},$$

which means that constant treatment A is just a mean value of periodic treatment.

Returning to Eqn. (18),

$$T((n+1)P) = T(nP)\cdot\exp\left(P - \frac{m}{A_{\text{crit}}}\right),$$

which corresponds to the Poincaré map

$$T((n+1)P) = F(T(nP)),$$

where

$$F(x) = x\,\mathrm{e}^{P-\frac{m}{A_{\mathrm{crit}}}}$$

and this map has a fixed point $x = 0$ which is stable under the condition (15). Using the same condition, it is possible to estimate the number of doses necessary to eradicate a tumour assuming its initial size $T_1(0)$ and arbitrary eradication size T_{er}. We need to find n such that

$$T_1(nP) = T_{\mathrm{er}},$$
$$T_1(nP) = T_1(0) \cdot \exp\left(n\left(P - \frac{m}{A_{\mathrm{crit}}}\right)\right),$$

yielding

$$n = \frac{\ln \frac{T_{\mathrm{er}}}{T_1(0)}}{P - \frac{m}{A_{\mathrm{crit}}}}.$$

Note, however, that this is the estimation for an approximation of Eqns. (2), while assuming constant treatment with specific parameter values it is possible to estimate numerically a basin of attraction for the semi-trivial steady state of Eqns. (2).

6. Parameters and numerical methods

To perform numerical simulations and optimise therapeutic schemes for the non-scaled model described by Eqns. (1), parameter values, estimated in several studies and summarised in Table 1 are used. These values imply that $\tilde{\rho}_C \tau_C > 1$, thus $\rho_C > \eta_C$, which ensures the existence of at least one non-negative steady state.

To study how the model parameters affect the model dynamics, a sensitivity analysis is performed. The dependence of the time taken for a tumour to reach a critical size on changes in a given parameter is studied. All other parameters are fixed and are taken at the left, middle and right ends of the ranges, see Table 1. The symbol '*' indicates the statistically significant correlation coefficients (p-value < 0.05). It needs to be highlighted that the correlation between the critical tumour size and the time it takes for the tumour to reach this value is almost linear. Thus, manipulating all but one parameter does not qualitatively change the result. Only a change in the parameter corresponding to the net growth rate of the tumour affects the result non-linearly.

The simulations performed assume that the initial tumour consists of 3.35×10^{10} cells while 2×10^7 CAR-T cells are assumed to be present in the tumour surroundings, representing the delivery of an initial dose and mimic the situation when the CAR-T treatment is started at time zero.

To solve the equations numerically, the standard MATLAB solver ode45 was used, with error tolerance equal to 10^{-9}. Finding the time when the solution reaches an assumed critical level was achieved by triggering the MATLAB event model with tolerance equal to 10^{-6}, while the time at which the control switch is to take place was obtained by solving the system with different switching times, increasing them until the predefined event occurs with prescribed tolerance and then by finding the appropriate switching time back. Statistical analysis was performed using R software based on the MATLAB numerical results.

7. Therapy controlling tumour size

This section illustrates the theoretical results using numerical simulations of the two treatments considered in this article, i.e., periodic (impulsive) and continuous. Moreover, therapy protocols are derived that keep tumours under control (below the assumed critical size), which is of paramount interest.

Theorems proved in the previous sections give conditions that guarantee the local stability of the tumour-free steady state. For the parameters presented in Table 1 the critical value is 1.14×10^7 CAR-T cells per day. However, in such a case, the tumour-free steady state is not globally stable and therapy may not be successful for tumours that are too large. Assuming the administration of an average dose of 2×10^7 CAR-T cells per day, the critical initial size of the tumour for which therapy is successful has been numerically calculated. It was assumed here that at the start of therapy no CAR-T cells were present in the patient organism. The results are presented in Fig. 3. In this case, periodic treatment is beneficial.

However, doses used in clinical practice are smaller, and the total number of CAR-T cells administered over the course of the therapy is limited. Thus, when dealing with an incurable tumour, it is reasonable to change the therapeutic goal from maximising the number of cells killed to maximising the patient survival time, defined as a maximal time when the tumour growth is controlled, meaning it remains below the assumed critical size. Therefore, the aim of the therapy would be to keep the tumour below a critical (or fatal) size and look for a dose administration scheme that achieves this goal. As mentioned earlier, the continuation of the previously initiated therapy is studied at the stage when the tumour size reaches the level of 3.35×10^{10} cells. At that point, the CAR-T population is assumed to have 2×10^7 cells. The critical size of the tumour was chosen arbitrarily to be 3.4×10^{10} cells. The total number of CAR-T cells to be administered during the entire treatment protocol is assumed to be limited to 3×10^8 cells. Nevertheless, manipulating these parameters does not affect the results qualitatively. For the particular values of the rest of the parameters, their ranges and the references, see Tab. 1.

Figure 4 shows the survival time and the cycle length plotted for periodic (impulsive) treatment for a fixed total number of administrated CAR-T cells, indicating that the

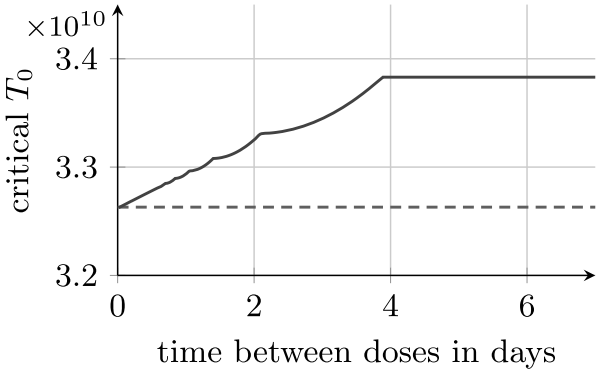

Fig. 3. Critical initial tumour size (T_0) that allows successful CAR-T cell therapy without restriction on therapy duration. The dashed line indicates continuous treatment, while the solid one shows the results for an impulsive (periodic) treatment. The average dose is the same in both the cases.

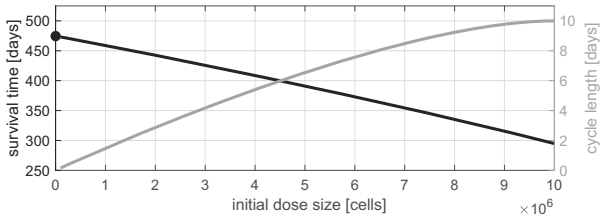

Fig. 4. Survival time and cycle length plotted against the initial dose size (which is equal to the periodic dose size) for a fixed total number of administrated CAR-T cells; here it is fixed as 3×10^8 cells. The point indicates the maximal survival time for a constant continuous treatment; here 473 days for 6.0405×10^5 cells.

Algorithm 1. Finding switching times.

Require: $size_{\text{crit}}$ {critical size of tumour}
Require: $init_{\text{cond}}$ {initial condition}
Require: $dose_{\max}$ {maximum single dose size administered continuously}
Require: $init_{\text{dose}}$, $init_{\text{duration}}$ {initial number of CAR-T cells to be administered and corresponding duration}
Require: $time_{\text{terminal}}$ {fixed terminal time for treatment}
Step 1. Find switch-on time
$time_{\text{start}} \leftarrow 0$ {dose administration start time}
while $\max(T) < size_{\text{crit}}$ **do**
  increase $time_{\text{start}}$
  $T \leftarrow$ **solve** model with $init_{\text{cond}}$, set $dose_{\max}$ for $time_{\text{start}} \le time \le time_{\text{terminal}}$
end while
return $time_{\text{start}}$ {switch-on time}
Step 2. Find switch-off time
$time_{\text{stop}} \leftarrow time_{\text{start}} + init_{\text{duration}}$ {switch-off time}
Step 3. Find switch-on and switch-off times
$[T, C] \leftarrow$ **solve** model with $init_{\text{cond}}$, set $dose_{\max}$ for $time_{\text{start}} \le time \le time_{\text{stop}}$
$init_{\text{cond}} \leftarrow [T, C]$ for $time_{\text{stop}}$
repeat Step 1
$time_{\text{stop}} \leftarrow time_{\text{start}}$
while $size_{\text{crit}} \le \max(T)$ **do**
  increase $time_{\text{stop}}$
  $T \leftarrow$ **solve** model with $init_{\text{cond}}$, set $dose_{\max}$ for $time_{\text{start}} \le time \le time_{\text{stop}}$
end while
return $time_{\text{stop}}$
Step 4.
repeat Step 3 **until** $time_{\text{stop}} \le time_{\text{terminal}}$

longest survival time is achieved with the smallest number of CAR-T cells administered and the shortest cycle length. As the cycle length decreases, the average number of CAR-T cells per unit time tends to the number of cells corresponding to a constant continuous treatment that results in the longest survival time.

A numerical study on optimising CAR-T cell administration to find a protocol that may prolong the maximal survival time more than periodic (impulsive) or constant continuous protocols is now presented. Bang-bang type protocols are considered, which is when the intervals of the maximal influx of CAR-T cells administration (with solutions' dynamics governed by (5)) are separated by time intervals when no treatment is given (the solution dynamics is governed by (2)). The total amount of cells administrated in one cycle (later called a periodic dose; see Fig. 5(d)) is defined as the maximum cell influx multiplied by the dosing time. Here, the maximum CAR-T cell influx is assumed to be equal to 2.8571×10^6 CAR-T cells per day or 2×10^7 CAR-T cells per 7 days. The time of the first dose administration (called later on initial injection time) is determined by a numerical optimisation algorithm in such a way as to prevent the tumour from reaching the critical value. The algorithm (see Algorithm 1) works as follows. For a specified fixed maximum single injection of cells, an initial time of treatment (first switching time) is found that will prevent the tumour from reaching the assumed critical size. Next, the initial injection (maximum single injection for a specific time) is administered. Then the next point in time to start continuous cell administration and the minimum CAR-T cells injection that will prevent the tumour from reaching the critical size is found. Finally, the last step is repeated.

The size of the initial CAR-T cell injection varies between simulations since it is also the subject of the optimisation. Figures 5(a) and (b) show the tumour (black solid line) and CAR-T (grey solid line) population dynamics for two different values of the initial CAR-T injection sizes, which are 7.2027×10^6 and 1×10^7 cells, respectively. The corresponding controls are depicted by

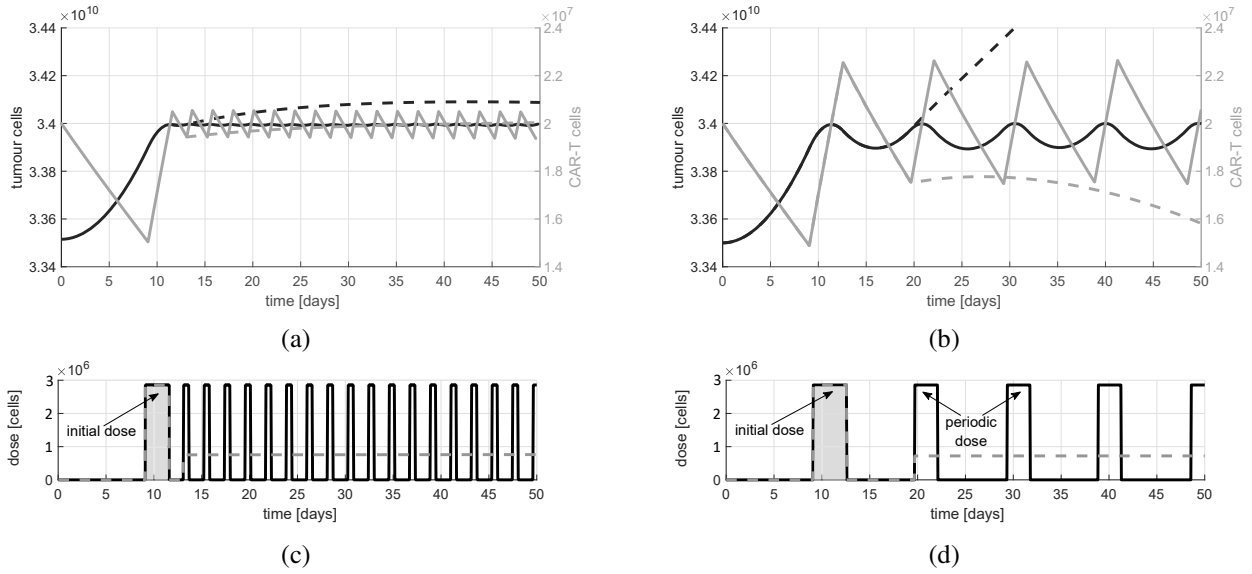

Fig. 5. Tumour and CAR-T size dynamics for initial dosing of 7.2027×10^6 cells injected over 2.5210 days (a) and of 1×10^7 cells injected over 3.5 days (b). The solid lines in panels (a) and (b) depict solutions for periodic treatments while in panels (c) and (d) they stand for the corresponding controls. The dashed lines in panels (a) and (b) indicate the solutions for treatment scheme with constant mean-value dose while in panels (c) and (d) they stand for the corresponding control. The mean doses are equal to (c) 7.6054×10^5 and (d) 7.2126×10^5 CAR-T cells per day.

black solid lines in Figures 5(c) and (d). One can see that after the initial dose administration, the treatment scheme preventing the tumour from reaching the critical value is periodic of the bang-bang type. Moreover, the size of the periodic dose and the length of the cycle are strongly dependent on the initial dose. Figures 5(a) and (b) compare the treatment outcome, for constant continuous treatment (dashed lines) and periodic (solid lines). The size of the constant dose is equal to the mean value of the periodic therapy dose (a ratio of the periodic dose to the length of the cycle). Figure 5(a) shows that with a relatively small initial dose, a constant treatment is able to control the size of the tumour (see dashed lines). However, the maximal allowable tumour size slightly crosses the assumed critical level. The amount of initially injected cells presented in Fig. 5(c) is the threshold value, as for smaller mean-value doses of the periodic therapy, tumour growth is out of control and grows exponentially (see dashed lines in Fig. 5(b)), while for larger mean-value of the periodic therapy doses, the solution goes to the semi-trivial steady state.

Figure 6 shows patient survival time plotted against the total amount of CAR-T cells administered and the size of the initial injection for numerically derived optimal bang-bang type treatment protocols. A number of simulations with different values of the initial dose and total amounts of CAR-T cells administrated were performed. For each of them, the corresponding lengths of the cycles (see the solid black curve in Fig. 7) and the size of the periodic dose were calculated and recorded. Then, the average number of injected cells per unit time was evaluated (the grey solid line in Fig. 7).

8. Conclusions and discussions

This article has described a mathematical model of the response of glioblastoma to CAR-T cell treatment, which takes into account the basic principles of interaction between these two kinds of cells. CAR-T cell-based immunotherapeutic treatments have been successfully used against certain types of leukaemias and lymphomas.

Starting from a general model, the focus was on exponential growth for the glioblastoma cells, and under that assumption, the mathematical properties of the considered model were studied analytically, including the existence and the stability of the steady states, as well as the absence of periodic solutions for the case where the therapy is represented as a single dose at the beginning of the treatment.

Next, focusing on a constant and periodic treatment for the system of differential equations, conditions were obtained that guaranteed control of the tumour, unlike the single dose case considered numerically by León-Triana *et al.* (2021) where the tumour finally regrew. Thus, the results indicate that the treatment for glioblastoma should not be a single dose of CAR-T cells, but constant or periodic doses over time, to keep the tumour under control.

Subsequently, a numerical approach was used to find other protocols to extend and improve the previous

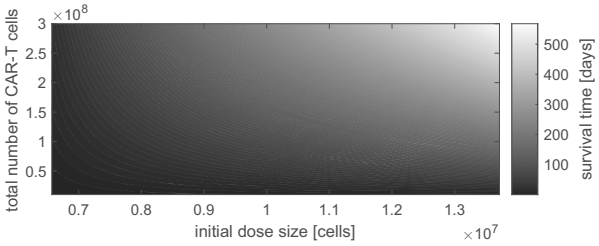

Fig. 6. Survival time plotted against the total amount of CAR-T cells administered and the size of the initial injection. Shading represents a maximal survival time, i.e., a maximal time when the tumour growth is controlled and remains below the critical size.

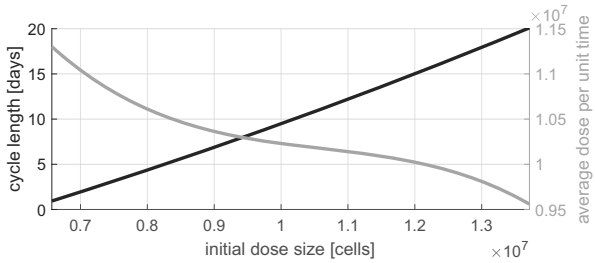

Fig. 7. Dependence of the cycle length and the average dose per unit time on the initial injection size for numerically estimated optimal bang-bang type treatment protocols.

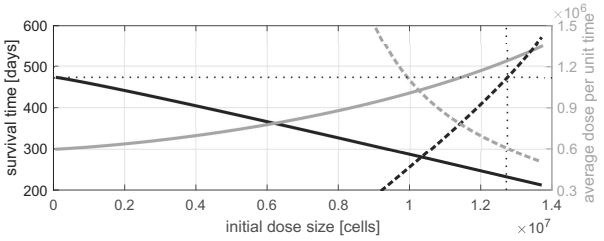

Fig. 8. Comparison of periodic and bang-bang type periodic administrations. The solid lines depict the survival time and the average amount of injected cells per unit time plotted against the number of initially injected cells, while dashed lines depict the survival time and the average number of injected cells per unit time plotted against the initially injected cells for bang-bang type periodic treatment. The dotted lines intersect at a point where both the types of treatment provide the same maximal survival time.

theoretical results. For this case, it was found that preventing the tumour from reaching a critical size leads to an eventually periodic dose administration scheme. The larger the first injection is, the larger the size of the periodic dose (i.e., the size of dose multiplied by the administration time) becomes with a lower average dose per unit time. When the initial injection is low, the average cost of periodic treatment, meaning it is the amount of CAR-T cells administered per injection in the periodic treatment scheme, is so high that the constant dosage is also able to control the tumour growth. This means that for small initial doses the periodic and constant schedules give similar results. As is shown in Fig. 7, for small initial injections, the average dose per unit time decreases in a concave manner. Thus, a slightly larger initial injection makes the average periodic dose too low to keep the tumour under control when administrated as a constant treatment. For larger initial doses, their changes affect the results much less significantly. Nevertheless, when the total number of administrated CAR-T cells (corresponding to the total cost of the treatment) is fixed, the longest survival time is achieved for the therapy scheme with the largest possible initial injection followed by a periodic scheme with the longest period between doses. Finally, it should be pointed out that the periodicity of the treatment is not assumed, but is a result of achieving the therapeutic goal.

Figure 8 presents a comparison of periodic and bang-bang type periodic administration protocols. There is a threshold for initially injected cells (i.e., single admission of periodically injected cells in the case of periodic treatment and in the case of bang-bang treatment the initial (first) dose that determines further part of the protocol) below which periodic dosing leads to longer survival times. However, for doses above the threshold, the bang-bang type periodic scheme gives better results than constant continuous and periodic treatments; here, the threshold initial dose was set to 1.2721×10^7 cells.

Since the study is limited to a minimalist model, several limitations are present within it. Spatial aspects are ignored which are necessary to explain the interaction between both types of cells (Pozzi *et al.*, 2022). Neither is cellular plasticity included, which is one of the main drivers of resistance to treatment (Yabo *et al.*, 2021). Other aspects, such as mutation of the tumour cells are assumed negligible and more complex treatment options such as combined therapies are not included in this study (Wang *et al.*, 2023). Furthermore, enriching the model with clinical data would give insights from a medical point of view.

Finally, future directions for this work can address the limitations previously mentioned. On the other hand, more complex models including dual target CAR-T cell therapy (León-Triana *et al.*, 2021) will also be studied subsequently.

Acknowledgment

J. Belmonte-Beitia and J.A. Romero-Rosales were supported by Junta de Comunidades de Castilla–La Mancha, Spain (grant no. SBPLY/19/180501/000211). J. Belmonte-Beitia was additionally supported by

Ministerio de Ciencia e Innovación, Spain (grant no. PID2019-110895RB-100). M. Bodnar, U. Foryś and M.J. Piotrowska were supported by the University of Warsaw through the project *Mathematical Modelling of Brain Tumours Growth Dynamics*, New Ideas 2B in Priority Research Area III in the framework of Excellence Initiative—Research University.

References

Anderson, K., Stromnes, I. and Greenberg, P. (2017). Obstacles posed by the tumor microenvironment to T cell activity: A case for synergistic therapies, *Cancer Cell* **31**(3): 311–325.

Bodnar, M. and Piotrowska, M.J. (2016). Stability analysis of the family of tumour angiogenesis models with distributed time delays, *Communications in Nonlinear Science and Numerical Simulation* **31**(1): 124–142.

Bodnar, M., Piotrowska, M.J. and Bogdańska, M.U. (2019). Mathematical analysis of a generalised model of chemotherapy for low grade gliomas, *Discrete and Continuous Dynamical Systems B* **24**(5): 2149–2167, DOI: 10.3934/dcdsb.2019088.

Bodzioch, M., Bajger, P. and Foryś, U. (2021). Angiogenesis and chemotherapy resistance: Optimizing chemotherapy scheduling using mathematical modeling, *Journal of Cancer Research and Clinical Oncology* **147**(8): 2281–2299, DOI: 10.1007/s00432-021-03657-9.

Brown, C.E., Alizadeh, D., Starr, R., Weng, L., Wagner, J.R., Naranjo, A., Ostberg, J.R., Blanchard, M.S., Kilpatrick, J., Simpson, J., Kurien, A., Priceman, S.J., Wang, X., Harshbarger, T.L., D'Apuzzo, M., Ressler, J.A., Jensen, M.C., Barish, M.E., Chen, M., Portnow, J., Forman, S.J. and Badie, B. (2016). Regression of glioblastoma after chimeric antigen receptor T-cell therapy, *New England Journal of Medicine* **375**(26): 2561–2569, DOI: 10.1056/NEJMoa1610497.

Castellarin, M., Watanabe, K., June, C.H., Kloss, C.C. and Posey, A.D. (2018). Driving cars to the clinic for solid tumors, *Gene Therapy* **25**(3): 165–175, DOI: 10.1038/s41434-018-0007-x.

Colli, P., Gomez, H., Lorenzo, G., Marinoschi, G., Reali, A. and Rocca, E. (2021). Optimal control of cytotoxic and antiangiogenic therapies on prostate cancer growth, *Mathematical Models and Methods in Applied Sciences* **31**(07): 1419–1468, DOI: 10.1142/S0218202521500299.

D'Agostino, M. and Raje, N. (2020). Anti-BCMA CAR T-cell therapy in multiple myeloma: Can we do better?, *Leukemia* **34**(1): 21–34, DOI: 10.1038/s41375-019-0669-4.

de Pillis, L., Gu, W., Fister, K., Head, T., Maples, K., Murugan, A., Neal, T. and Yoshida, K. (2007). Chemotherapy for tumors: An analysis of the dynamics and a study of quadratic and linear optimal controls, *Mathematical Biosciences* **209**(1): 292–315,

D'Errico, G., Machado, H.L. and Sainz Jr., B. (2017). A current perspective on cancer immune therapy: Step-by-step approach to constructing the magic bullet, *Clinical and Translational Medicine* **6**(1): e3, DOI: abs/10.1186/s40169-016-0130-5.

Feins, S., Kong, W., Williams, E.F., Milone, M.C. and Fraietta, J.A. (2019). An introduction to chimeric antigen receptor (car) T-cell immunotherapy for human cancer, *American Journal of Hematology* **94**(S1): S3–S9, DOI: 10.1002/ajh.25418.

Foryś, U. and Marciniak-Czochra, A.K. (2003). Logistic equations in tumour growth modelling, *International Journal of Applied Mathematics and Computer Science* **13**(3): 317–325.

Garcke, H., Lam, K.-F. and Rocca, E. (2018). Optimal control of treatment time in a diffuse interface model of tumor growth, *Applied Mathematics & Optimization* **78**: 495–544, DOI: 10.1007/s00245-017-9414-4.

Ghorashian, S., Kramer, A., Onuoha, S., Wright, G., Bartram, J., Richardson, R., Albon, S.J., Casanovas-Company, J., Castro, F., Popova, B., Villanueva, K., Yeung, J., Vetharoy, W., Guvenel, A., Wawrzyniecka, P.A., Mekkaoui, L., Cheung, G.W.-K., Pinner, D., Chu, J., Lucchini, G., Silva, J., Ciocarlie, O., Lazareva, A., Inglott, S., Gilmour, K.C., Ahsan, G., Ferrari, M., Manzoor, S., Champion, K., Brooks, T., Lopes, A., Hackshaw, A., Farzaneh, F., Chiesa, R., Rao, K., Bonney, D., Samarasinghe, S., Goulden, N., Vora, A., Veys, P., Hough, R., Wynn, R., Pule, M.A. and Amrolia, P.J. (2019). Enhanced car T cell expansion and prolonged persistence in pediatric patients with all treated with a low-affinity cd19 car, *Nature Medicine* **25**(5): 1408–1414.

Hege, K.M., Bergsland, E.K., Fisher, G.A., Nemunaitis, J.J., Warren, R.S., McArthur, J.G., Lin, A.A., Schlom, J., June, C.H. and Sherwin, S.A. (2017). Safety, tumor trafficking and immunogenicity of chimeric antigen receptor (CAR)-T cells specific for TAG-72 in colorectal cancer, *Journal for ImmunoTherapy of Cancer* **5**(1): 22, DOI: 10.1186/s40425-017-0222-9.

Koury, J., Lucero, M., Cato, C., Chang, L., Geiger, J., Henry, D., Hernandez, J., Hung, F., Kaur, P., Teskey, G. and Tran, A. (2018). Immunotherapies: Exploiting the immune system for cancer treatment, *Journal of Immunology Research* **2018**: 9585614, DOI: 10.1155/2018/9585614.

León-Triana, O., Perez-Martinez, A., Ramirez-Orellana, M. and Perez-Garcia, V. (2021). Dual-target CAR-TS with on- and off-tumour activity may override immune suppression in solid cancers: A mathematical proof of concept, *Cancers* **13**(4): 703, DOI: 10.3390/cancers13040703.

Lima, E.A., Wyde, R., Sorace, A.G. and Yankeelov, T.E. (2022). Optimizing delivery of combination targeted and chemotherapy in a murine model of HER2+ breast cancer, *Cancer Research* **82**(12 Supplement): 5050–5050, DOI: 10.1158/1538-7445.AM2022-5050.

Locke, F.L., Ghobadi, A., Jacobson, C.A., Miklos, D.B., Lekakis, L.J., Oluwole, O.O., Lin, Y., Braunschweig, I., Hill, B.T., Timmerman, J.M., Deol, A., Reagan, P.M., Stiff, P., Flinn, I.W., Farooq, U., Goy, A., McSweeney, P.A., Munoz, J., Siddiqi, T., Chavez, J.C., Herrera, A.F., Bartlett, N.L., Wiezorek, J.S., Navale, L., Xue, A., Jiang,

Y., Bot, A., Rossi, J.M., Kim, J.J., Go, W.Y. and Neelapu, S.S. (2019). Long-term safety and activity of axicabtagene ciloleucel in refractory large B-cell lymphoma (ZUMA-1): A single-arm, multicentre, phase 1-2 trial, *The Lancet Oncology* **20**(1): 31–42.

Mahlbacher, G.E., Reihmer, K.C. and Frieboes, H.B. (2019). Mathematical modeling of tumor-immune cell interactions, *Journal of Theoretical Biology* **469**: 47–60, DOI: 10.1016/j.jtbi.2019.03.002.

Maude, S.L., Laetsch, T.W., Buechner, J., Rives, S., Boyer, M., Bittencourt, H., Bader, P., Verneris, M.R., Stefanski, H.E., Myers, G.D., Qayed, M., De Moerloose, B., Hiramatsu, H., Schlis, K., Davis, K.L., Martin, P.L., Nemecek, E.R., Yanik, G.A., Peters, C., Baruchel, A., Boissel, N., Mechinaud, F., Balduzzi, A., Krueger, J., June, C. H., Levine, B.L., Wood, P., Taran, T., Leung, M., Mueller, K.T., Zhang, Y., Sen, K., Lebwohl, D., Pulsipher, M.A. and Grupp, S.A. (2018). Tisagenlecleucel in children and young adults with B-cell lymphoblastic leukemia, *New England Journal of Medicine* **378**(5): 439–448, DOI: 10.1056/NEJMoa1709866.

Miliotou, N.A. and Papadopoulou, C.L. (2018). CAR T-cell therapy: A new era in cancer immunotherapy, *Current Pharmaceutical Biotechnology* **19**(1): 5–18.

Mostolizadeh, R., Afsharnezhad, Z. and Marciniak-Czochra, A. (2018). Mathematical model of chimeric anti-gene receptor (CAR) T cell therapy with presence of cytokine, *Numerical Algebra, Control and Optimization* **8**(1): 63–80.

Pérez-García, V., Calvo, G., Bosque, J., León-Triana, O., Jiménez SĂˇnchez, J., Pérez Beteta, J., Belmonte-Beitia, J., Valiente, M., Zhu, L., García Gómez, P., Sánchez-Gómez, P., Miguel, E., Hortiguela, R., Azimzade, Y., Molina-García, D., Martínez-Rubio, A., Rojas, A., Ortiz de Mendivil, A., Vallette, F. and Vicente, A. (2020). Universal scaling laws rule explosive growth in human cancers, *Nature Physics* **16**(12): 1–6, DOI: 10.1038/s41567-020-0978-6.

Pérez-García, V.M. and Pérez-Romasanta, L.A. (2015). Extreme protraction for low-grade gliomas: Theoretical proof of concept of a novel therapeutical strategy, *Mathematical Medicine and Biology: A Journal of the IMA* **33**(3): 253–271, DOI: 10.1093/imammb/dqv017.

Pozzi, G., Grammatica, B., Chaabane, L., Catucci, M., Mondino, A., Zunino, P. and Ciarletta, P. (2022). T cell therapy against cancer: A predictive diffuse-interface mathematical model informed by pre-clinical studies, *Journal of Theoretical Biology* **547**: 111172, DOI: 10.1016/j.jtbi.2022.111172.

Radunskaya, A., Kim, R. and Woods, T. (2018). Mathematical modeling of tumor immune interactions: A closer look at the role of a PD-l1 inhibitor in cancer immunotherapy, *Spora: A Journal of Biomathematics* **4**: 25–41, DOI: 10.30707/SPORA4.1Radunskaya.

Sahoo, P., Yang, X., Abler, D., Maestrini, D., Adhikarla, V., Frankhouser, D., Cho, H., Machuca, V., Wang, D., Barish, M., Gutova, M., Branciamore, S., Brown, C.E. and Rockne, R.C. (2020). Mathematical deconvolution of CAR T-cell proliferation and exhaustion from real-time killing assay data, *Journal of The Royal Society Interface* **17**(162): 20190734, DOI: 10.1098/rsif.2019.0734.

Sancho-Araiz, A., Mangas-Sanjuan, V. and Trocóniz, I.F. (2021). The role of mathematical models in immuno-oncology: Challenges and future perspectives, *Pharmaceutics* **13**(7): 1016.

Schuster, S.J., Bishop, M.R., Tam, C.S., Waller, E.K., Borchmann, P., McGuirk, J.P., Jäger, U., Jaglowski, S., Andreadis, C., Westin, J.R., Fleury, I., Bachanova, V., Foley, S.R., Ho, P.J., Mielke, S., Magenau, J.M., Holte, H., Pantano, S., Pacaud, L.B., Awasthi, R., Chu, J., Anak, O., Salles, G. and Maziarz, R.T. (2019). Tisagenlecleucel in adult relapsed or refractory diffuse large B-cell lymphoma, *New England Journal of Medicine* **380**(1): 45–56, DOI: 10.1056/NEJMoa1804980.

Shah, N.N. and Fry, T.J. (2019). Mechanisms of resistance to CAR T cell therapy, *Nature Reviews Clinical Oncology* **16**(6): 372–385, DOI: 10.1038/s41571-019-0184-6.

Stein, A.M., Grupp, S.A., Levine, J.E., Laetsch, T.W., Pulsipher, M.A., Boyer, M.W., August, K.J., Levine, B.L., Tomassian, L., Shah, S., Leung, M., Huang, P.-H., Awasthi, R., Mueller, K.T., Wood, P.A. and June, C.H. (2019). Tisagenlecleucel model-based cellular kinetic analysis of chimeric antigen receptor-T cells, *CPT: Pharmacometrics & Systems Pharmacology* **8**(5): 285–295, DOI: abs/10.1002/psp4.12388.

Stein, S., Zhao, R., Haeno, H., Vivanco, I. and Michor, F. (2018). Mathematical modeling identifies optimum lapatinib dosing schedules for the treatment of glioblastoma patients, *PLOS Computational Biology* **14**(1): 1–24, DOI: 10.1371/journal.pcbi.1005924.

Stensjoen, A., Solheim, O., Kvistad, K., Haberg, A., Salvesen, O. and Berntsen, E. (2015). Growth dynamics of untreated glioblastomas in vivo, *Neuro-Oncology* **17**(10): 1402–1411, DOI: 10.1093/neuonc/nov029.

Świerniak, A., Ledzewicz, U. and Schättler, H. (2003). Optimal control for a class of compartmental models in cancer chemotherapy, *International Journal of Applied Mathematics and Computer Science* **13**(3): 357–368.

Wang, A.X., Ong, X.J., D'Souza, C., Neeson, P.J. and Zhu, J.J. (2023). Combining chemotherapy with CAR-T cell therapy in treating solid tumors, *Frontiers in Immunology* **14**: 1140541, DOI: 10.3389/fimmu.2023.1140541.

Yabo, Y.A., Niclou, S.P. and Golebiewska, A. (2021). Cancer cell heterogeneity and plasticity: A paradigm shift in glioblastoma, *Neuro-Oncology* **24**(5): 669–682, DOI: 10.1093/neuonc/noab269.

Marek Bodnar is an associate professor with the Institute of Applied Mathematics and Mechanics, Faculty of Mathematics, Informatics and Mechanics, University of Warsaw. He is interested in the application of dynamical systems (mainly delay and differential equations, but also partial differential equations) in the modelling of biological and medical phenomena, in particular tumour growth, tumour-immune system interactions as well as anticancer therapies.

Urszula Foryś is a professor of mathematics at the Institute of Applied Mathematics and Mechanics, University of Warsaw (UW). She holds a PhD in applied mathematics from the UW and a habilitation from the Institute of Biocebernetics and Biomedical Engineering, PAS. She is an expert in the mathematical modelling of biomedical phenomena, mainly related to tumour growth and treatment, and eco-epidemiological modelling, as well as dyadic interactions and neuroscience.

Monika J. Piotrowska is an associate professor at the Institute of Applied Mathematics and Mechanics, University of Warsaw. In 2016 she obtained a habilitation in mathematics. She is interested in the mathematical and computational modelling of various natural phenomena, including tumour growth, angiogenesis, tumour-immune system interactions, transmissions of pathogens within hospitals, investigation of anticancer therapies and infection control strategies.

Mariusz Bodzioch is a graduate in mathematics and computer science and obtained a PhD in mathematics in 2017 at the University of Warmia and Mazury in Olsztyn, Poland. His research focuses on mathematical models of infectious disease dynamics and mathematical models of tumour growth, in particular modelling drug resistance, angiogenesis, and applications of optimal control theory to therapy scheduling.

Jose A. Romero Rosales holds a BS in physics from Universidad de Còrdoba and an MA in physics and mathematics (biomathematics and bioinformatics) from Universidad de Castilla–La Mancha. He is currently a PhD candidate there. His research includes partial differential equations applied to mathematical oncology and medical image analysis.

Juan Belmonte-Beitia is a graduate in mathematics and physics from Universidad Complutense de Madrid and holds a PhD in mathematics (2008) from the University of Castilla–La Mancha. His research interests are dynamical systems, differential equations and partial differential equations as well as their applications to mathematical biology, specifically the mathematical modelling of tumour growth.

Received: 12 October 2022
Revised: 27 February 2023
Re-revised: 12 May 2023
Accepted: 15 May 2023